PRE-PUBLICACIONES del seminario matematico "garcia de galdeano"

2005

Quadratic Hamiltonians on nonsymmetric Poisson structures

M. Arribas
F. Blesa
A. Elipe

n. 1

seminario matemático
garcía de galdeano
Universidad de Zaragoza

QUADRATIC HAMILTONIANS ON NONSYMMETRIC POISSON STRUCTURES

M. ARRIBAS*, F. BLESA†, AND A. ELIPE‡

Abstract. Many dynamical systems may be represented in a set of non-canonical coordinates that generate an su(2) algebraic structure. The topology of the phase space is the one of the S^2 sphere, the Poisson structure is the one of the rigid body, and the Hamiltonian is a parametric quadratic form in these "spherical " coordinates. However, there are other problems in which the Poisson structure losses its symmetry. In this paper we analyze this case and, we show how the loss of the spherical symmetry affects the phase flow and parametric bifurcations for the bi-parametric cases.

Key words. Bifurcations; Poisson structure; Parametric Hamiltonians

AMS subject classifications. 58F14, 34C23, 70H05

1. Introduction. There are some dynamical systems represented by a Hamiltonian that is a quadratic function in a set of non canonical variables that generate an su(2) algebraic structure. In these variables the system has a singular noncanonical bracket tensor, and a conserved quantity, called *Casimir*, exists due to the degeneracy of the bracket [26, 27]. The topology of the phase space is defined by a constant-energy sphere (Hopf sphere). The representation on the sphere presents several advantages, among them that it is a geometrical figure easy to plot and that the phase portrait may be obtained as the intersection of the two surfaces, the quadratic function and the sphere, with no need of numerical integration for several values of the energy constant.

We find this type of problem in classical mechanics, e.g. in the rigid body in torque free motion [1, 2, 3, 10], the most representative and one of the simplest cases. Indeed, by denoting by u, v and w the components of the angular momentum $\boldsymbol{G}$ in the body frame, there results that its norm is an integral, thus we have that the sough Casimir is the sphere $u^2+v^2+w^2=G^2$, and the energy —or the Hamiltonian in this case— is the quadratic form $H=\frac{1}{2}(a_1u^2+a_2v^2+a_3w^2)$, where a_i are the reciprocal of the moments of inertia. In this case, the quadratic form is very simple: a triaxial ellipsoid. The non canonical brackets tensor [26] is

$$\begin{pmatrix} 0 & -w & v \\ w & 0 & -u \\ -v & u & 0 \end{pmatrix},$$

and the Poisson structure [10] is given by the relations

$$\{u,v\}=-w, \qquad \{v,w\}=-u, \qquad \{w,u\}=-v. \tag{1.1}$$

Quadratic Hamiltonians on the S^2 sphere also appear as a representation of the phase flow of perturbed elliptic oscillators obtained after a normalization [8, 9, 13, 28]. It was proven [29] that the reduced phase space in Hopf coordinates is a sphere. In

*Grupo de Mecánica Espacial. Dpto. Matemática Aplicada. Universidad de Zaragoza. 50009 Zaragoza. Spain

†Grupo de Mecánica Espacial, Dpto. Física Aplicada. Escuela Politécnica de Huesca. Universidad de Zaragoza. Huesca. Spain

‡Grupo de Mecánica Espacial. Universidad de Zaragoza. 50009 Zaragoza. Spain

this context we find this structure in the motion of atoms in electric and magnetic fields [20, 30, 14]; in studies on molecules [16, 17]; in the context of Hamiltonian chaos in nonlinear optical polarization dynamics [6, 7]; in the detection of frozen orbits in the artificial satellite theory [5]; and in galactic dynamics [4, 9, 15] among others.

The above mentioned problems belong to the class of Hamiltonians of the type

$$H = H(u, v, w; \boldsymbol{\alpha}),$$

with the variables lying on the sphere

$$S^2 \equiv u^2 + v^2 + w^2 = 1 \tag{1.2}$$

and the Poisson structure (1.1), where $\boldsymbol{\alpha} \in \mathbb{R}^n$ are real parameters.

Lanchares and Elipe [22] and later on Frauendiener [19] proceeded to classify all possible parametric quadratic Hamiltonians

$$H = au^2 + bv^2 + cw^2 + 2fuv + 2guw + 2hvw + lu + mv + nw \tag{1.3}$$

with the above Poisson structure (1.1). By virtue of the spherical symmetry, both the Hamiltonian and the Poisson brackets enjoy properties like the invariance by translations, rotations and time reversing, which reduce the possibilities to only the five cases given in Table 1.1

No. parameters	Hamiltonian
1	$H = \frac{1}{2}u^2 + Rv$
2.a	$H = \frac{1}{2}u^2 + Qu + Rv$
2.b	$H = \frac{1}{2}u^2 + \frac{1}{2}Pv^2 + Qu$
3	$H = \frac{1}{2}u^2 + \frac{1}{2}Pv^2 + Qu + Rv$
4	$H = \frac{1}{2}u^2 + \frac{1}{2}Pv^2 + Qu + Rv + Sw$

TABLE 1.1
Possible Hamiltonian cases depending on the number of parameters

The determination of parametric bifurcations and the evolution of the phase flow for cases 1, 2.a, 2.b and 3 was done by Elipe and coworkers [23, 24, 25].

Incidentally, let us mention that the problem of the gyrostat in free motion is the most general case belonging to this kind of Hamiltonians [12]. Indeed, the expression of the Hamiltonian for this problem is

$$H = \frac{1}{2}(a_1u^2 + a_2v^2 + a_3w^2) - (a_1f_1u + a_2f_2v + a_3f_3w)$$

where u, v, w are the components of the total angular momentum, and f_i the components of the angular momentum of the rotors, both expressed in the system of principal axes of inertia. In this system the angular momentum vector is an integral, and the Poisson structure is the one given in Eq. (1.1).

Hamiltonians of the class (1.3) on the sphere with the Poisson structure (1.1) appear also in several physical problems, and among them, the problem of normalized

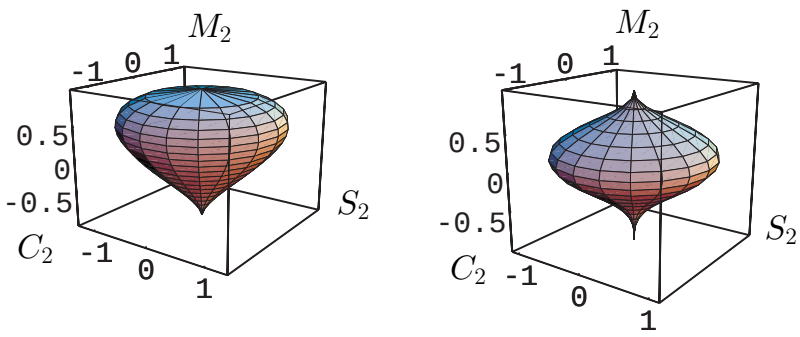

FIG. 1.1. *Phase space on pinched spheres. Left* $p = 1, q = 3$*; right* $p = 2, q = 3$.

harmonic oscillators in resonance 1:1. But, there are problems (for instance, the motion of a star under the field of an elliptic galaxy [4], of the classical Fermi resonance [18]) where the resonance is p:q, with p, q coprime integers. For this resonant case the topology of the phase flow [21, 11] is one-pinched sphere if $p = 1, q \neq 1$, a two-pinched sphere if both $p, q \neq 1$ and a sphere when $p = q = 1$. These *spheres* can be represented in a set of Cartesian coordinates $(C_2, S_2, M_2) \in \mathbb{R}^3$ by

$$C_2^2 + S_2^2 = (M_1 + M_2)^q \, (M_1 - M_2)^p,$$

where $M_1 \in \mathbb{R}$ is a positive constant, and $|M_2| \leq M_1$ (see Figure 1.1).

The Poisson structure for the above non canonical variables is given by the relations:

$$\{M_2; C_2\} = pqS_2, \quad \{C_2; S_2\} = pq\, f(M_2), \quad \{S_2; M_2\} = pqC_2, \tag{1.4}$$

with $f(M_2) = \frac{1}{2}(M_1 + M_2)^{q-1}(M_1 - M_2)^{p-1}[(q + p)M_2 + (p - q)M_1]$.

The Casimir is now (see [11] for details)

$$C_2^2 + S_2^2 = (M_1 + M_2)^q \, (M_1 - M_2)^p, \tag{1.5}$$

precisely, the above mentioned *pinched sphere*. From here on, the integral M_1 will be taken equal to the unit.

It can be shown by straightforward computation than in this case there is no spherical symmetry; the Poisson structure is not preserved by the rotation group SO(3) but just by rotations about the M_2 axis and, consequently, the classification of the possible cases depending on the number of parameters is more complex than in the classical case. Notwithstanding with this classification, we will present how this lack of symmetry affects the parametric bifurcations in some particular cases; in particular, we will only consider the biparametric case.

The paper is estructured as follows: In Section 2 we consider the cases 2.a and 2.b of the Table 1.1 with the new Poisson structure. We will see that both cases are quite similar to the classical ones. In Section 3 we analyze two new cases, and determine the bifurcation lines on the parameters plane. The results show that the variety of possible equilibria and bifurcations is much richer than the classical cases.

2. Biparametric case: Two known examples. For quadratic Hamiltonians on the sphere (1.2) with the Poisson structure (1.1), Lanchares and Elipe [23, 24] proved that there are two and only two independent Hamiltonians, the ones dubbed as 2.a and 2.b in Table 1.1. Now, a question is in order. What happens when the quadratic Hamiltonian is on the revolution surface (1.5) with the structure (1.4) with $1 \leq p < q$?. In other words, how does the loss of spherical symmetry affect the equilibria and bifurcations?

Because of the invariance by rotations about M_2, we can get rid of the mixed term C_2S_2, and since we are dealing with quadratic Hamiltonians, not all quadratic terms vanish, then, we can assume that one of the parameters is equal to the unit. Therefore, the possible bi-parametric Hamiltonians are listed on Table 2.1.

$H_1 = C_2^2 + AS_2^2 + BM_2^2$	$H_{16} = C_2^2 + 2AS_2M_2 + BM_2$
$H_2 = C_2^2 + AS_2^2 + 2BC_2M_2$	$H_{17} = C_2^2 + AC_2 + BS_2$
$H_3 = C_2^2 + AS_2^2 + BC_2$	$H_{18} = C_2^2 + AC_2 + BM_2$
$H_4 = C_2^2 + AS_2^2 + BM_2$	$H_{19} = C_2^2 + AS_2 + BM_2$
$H_5 = C_2^2 + AM_2^2 + 2BC_2M_2$	$H_{20} = M_2^2 + 2AC_2M_2 + 2BS_2M_2$
$H_6 = C_2^2 + AM_2^2 + 2BS_2M_2$	$H_{21} = M_2^2 + 2AC_2M_2 + BC_2$
$H_7 = C_2^2 + AM_2^2 + BC_2$	$H_{22} = M_2^2 + 2AC_2M_2 + BS_2$
$H_8 = C_2^2 + AM_2^2 + BS_2$	$H_{23} = M_2^2 + 2AC_2M_2 + BM_2$
$H_9 = C_2^2 + AM_2^2 + BM_2$	$H_{24} = M_2^2 + AC_2 + BM_2$
$H_{10} = C_2^2 + 2AC_2M_2 + 2BS_2M_2$	$H_{25} = C_2M_2 + AS_2M_2 + BC_2$
$H_{11} = C_2^2 + 2AC_2M_2 + BC_2$	$H_{26} = C_2M_2 + AS_2M_2 + BS_2$
$H_{12} = C_2^2 + 2AC_2M_2 + BS_2$	$H_{27} = C_2M_2 + AS_2M_2 + BM_2$
$H_{13} = C_2^2 + 2AC_2M_2 + BM_2$	$H_{28} = C_2M_2 + AC_2 + BS_2$
$H_{14} = C_2^2 + 2AS_2M_2 + BC_2$	$H_{29} = C_2M_2 + AC_2 + BM_2$
$H_{15} = C_2^2 + 2AS_2M_2 + BS_2$	$H_{30} = C_2M_2 + AS_2 + BM_2$

TABLE 2.1

Possible bi-parametetric quadratic Hamiltonians.

By analogy with the sphere, we will denote north and south poles the points $(0, 0, +1)$ and $(0, 0, -1)$, respectively. By equator we mean the maximum circle perpendicular to the axis of rotation M_2:

$$C_2^2 + S_2^2 = R^2, \qquad M_2 = \frac{q-p}{p+q};$$

its radius R is given by

$$R^2 = 2^{p+q}\left(\frac{p}{p+q}\right)^p\left(\frac{q}{p+q}\right)^q. \tag{2.1}$$

For the Hamiltonians,

$$H = \frac{1}{2}C_2^2 + \frac{1}{2}AS_2^2 + BC_2, \tag{2.2}$$

$$H = \frac{1}{2}C_2^2 + AC_2 + BS_2, \tag{2.3}$$

some of the results here obtained are analogous to the ones studied in [23, 24], but not exactly the same, as we will show.

2.1. Case $H = \frac{1}{2}C_2^2 + \frac{1}{2}AS_2^2 + BC_2$**.** For this case, by virtue of Liouville theorem ($\dot{F} = \{H\,;\,F\}$), the equations of motion are

$$\begin{aligned}
\dot{C}_2 = \{H\,;\,C_2\} &= -\frac{1}{2}A(1-M_2)^{-1+p}(1+M_2)^{-1+q} \\
&\quad \times\Big[p(1+M_2) - q(1-M_2)\Big]pqS_2, \\
\dot{S}_2 = \{H\,;\,S_2\} &= \frac{1}{2}(B+C_2)(1-M_2)^{-1+p}(1+M_2)^{-1+q} \\
&\quad \times\Big[p(1+M_2) - q(1-M_2)\Big]pq, \\
\dot{M}_2 = \{H\,;\,M_2\} &= -[B + C_2 - AC_2]pqS_2.
\end{aligned}$$

We are looking for equilibria of this system with the constraint (1.5) since the points must lie on the surface.

Note that the above equations are invariant by the symmetry

$$(B, C_2, t) \mapsto (-B, -C_2, -t),$$

thus, the bifurcation will be symmetric with respect to the axis $A = 0$, and if a point (C_2, S_2, M_2) is of equilibrium, its symmetric one $(-C_2, S_2, M_2)$ is also equilibrium.

For $A = 0$ and $C_2 = -B$, the above three equations vanish; therefore the closed curve

$$\begin{cases} C_2 = -B, \qquad S_2^2 = -B^2 + (1+M_2)^q(1-M_2)^p, \\ \text{and} \quad -R \le B \le +R \end{cases}$$

is made of equilibria, resulting, hence, a degeneracy. Note that the bound R for the value B comes from the fact that the both C_2, S_2 are, at most, equal to the radius R above defined (2.1).

On the other hand, for $A = 1$, $B = 0$, the equator is made of equilibria.

Besides these particular cases, the isolated equilibria are of four kinds, namely, points on the equator and $S_2 = 0$

$$E_{2,4} = \left(\pm R, 0, -\frac{p-q}{p+q}\right);$$

points on the equator and $S_2 \neq 0$

$$E_e = \left(\frac{B}{A-1}, S_{2e}, -\frac{p-q}{p+q}\right);$$

with

$$\left|\frac{B}{A-1}\right| < R \quad \text{and} \quad S_{2e} = \pm\sqrt{R^2 - \left(\frac{B}{A-1}\right)^2}.$$

Points on the meridian $E_m = (-B, 0, M_{2m})$, with $|B| < R$, and M_{2m} the roots of the equation $(1+M_2)^q\,(1-M_2)^p = B^2$.

Lastly, the south pole $E_s = (0, 0, -1)$ is equilibrium everywhere since it is a singular point in the phase space. Note also that if $p > 1$, the north pole $E_n = (0, 0, 1)$ is equilibrium everywhere.

The bifurcation lines are quite similar to the classical case ($p = q = 1$), but now the value R plays a important role, as we just shown. Note that in the classical case, $R = 1$. In Figure 2.1, the parallel lines correspond to $B = \pm R$ and the crossing lines to $B = \pm R\,(A-1)$. In the particular case $p = q = 1$ we have the same parametric plane obtained by Lanchares and Elipe [24].

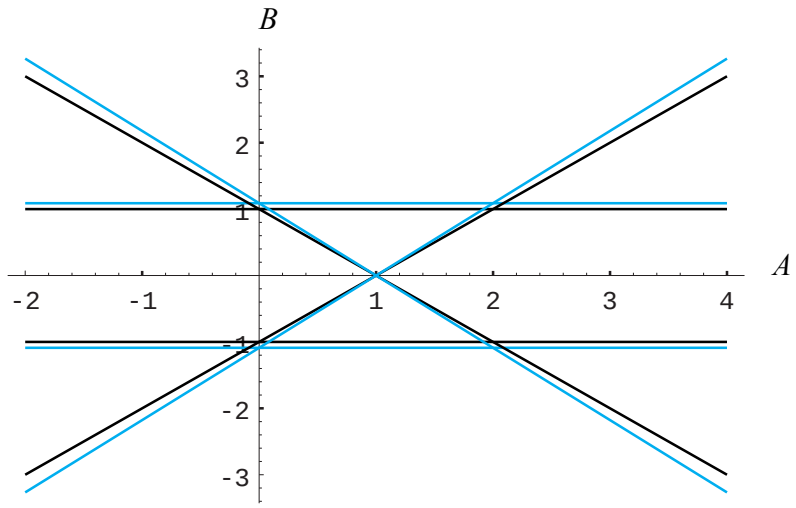

FIG. 2.1. *Bifurcation lines in the parametric plane AB for the Hamiltonian (2.2). In black the case for $p = q = 1$; in grey the case for $p = 1, q = 2$. The vertical segment $A = 0$, $|B| \leq R$, corresponds to non-isolated equilibria.*

2.2. Case $H = \frac{1}{2}C_2^2 + AC_2 + BS_2$**.** For this case, the equations of motion are

$$\dot{C}_2 = -\tfrac{1}{2}B(1-M_2)^{-1+p}(1+M_2)^{-1+q}[p(1+M_2) - q(1-M_2)]pq,$$

$$\dot{S}_2 = \tfrac{1}{2}(A+C_2)(1-M_2)^{-1+p}(1+M_2)^{-1+q}[p(1+M_2) - q(1-M_2)]pq,$$

$$\dot{M}_2 = pq[BC_2 - (A+C_2)S_2].$$

These equations are invariant by the symmetry $(A, C_2, t) \mapsto (-A, -C_2, -t)$.

For this system, together with the constraint (1.5), we find that the north and south poles $(0, 0, \pm 1)$ make zero the system (provided $p > 1$, otherwise the point $(0, 0, +1)$ is not solution).

When the parameter $B = 0$, we have two types of equilibria.

On the one hand, the points on the equator

$$\left(\pm R, 0, -\frac{p-q}{p+q}\right),$$

are equilibria and, on the other, all points on the closed curve

$$\begin{cases} C_2 = -A, \quad S_2^2 = -A^2 + (1+M_2)^q(1-M_2)^p, \\ \text{with} \quad -R \leq A \leq +R \end{cases}$$

are equilibria. We have thus a degeneracy.

If $B \neq 0$, there are equilibria on the equator. Indeed, for this value of M_2, the first two equations of the motion vanish, and the third one is equal to zero for $S_2 = BC_2/(A+C_2)$. But the point must be on the surface (1.5), hence, its coordinate C_2 must be a root of the quadratic equation

$$B^2C_2^2 + (A+C_2)^2(C_2^2 - R^2) = 0. \tag{2.4}$$

For the classical case ($p = q = 1$), Lanchares and Elipe [23] obtained that the above equation (with $R^2 = 1$) had either 2 or 3 or 4 roots (equivalently 2, 3 or 4 equilibria) depending on whether the values of the parameters A and B are, respectively, in the interior, on the curve or the exterior of the astroid $A^{2/3} + B^{2/3} = 1$.

By the same token, one can prove that for the general values of p and q, the bifurcation curve on the parametric plane A, B is the astroid or the four-cusps-hypocycloid $A^{2/3} + B^{2/3} = R^{2/3}$. This situation is shown in Figure 2.2.

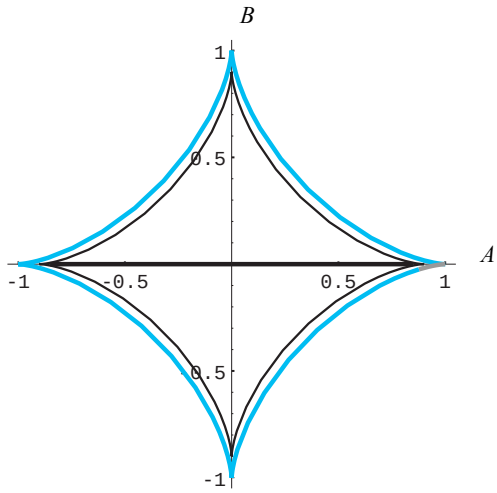

FIG. 2.2. *Bifurcation lines in the parametric plane A, B for the Hamiltonian (2.3). In grey the case for $p = q = 1$; in black the case for $p = 1, q = 2$. The horizontal segment $B = 0$, $-R \leq A \leq R$ corresponds to the degenerate case (non-isolated equilibria).*

3. Biparametric case: Two new samples.

3.1. Two quadratic terms plus a linear one. Let us take the following Hamiltonian made by two quadratic terms plus a linear one:

$$H = \frac{1}{2}C_2^2 + \frac{1}{2}AS_2^2 + BM_2. \tag{3.1}$$

Since there is spherical symmetry neither on the surface (1.5) nor in the Poisson structure (1.4), this problem is not equivalent to the previous ones. Hence, one should expect that the number of equilibria and the partition of the parametric plane would be different to the case 2.1.

The equations of the motion are now

$$\begin{aligned}
\dot{C}_2 &= \frac{pq}{2(1-M_2^2)} \\
&\quad \times\Big\{2B(1-M_2^2) - A(1-M_2)^p(1+M_2)^q\Big[p(1+M_2) - q(1-M_2)\Big]\Big\}S_2, \\
\dot{S}_2 &= -\frac{pq}{2(1-M_2^2)} \\
&\quad \times\Big\{2B(1-M_2^2) + (1-M_2)^p(1+M_2)^q\Big[p(1+M_2) - q(1-M_2)\Big]\Big\}C_2, \\
\dot{M}_2 &= (-1+A)\,pq\,C_2S_2.
\end{aligned}$$

Since for the time being we are interested in showing the differences of this new Hamiltonian with the previous ones, we restrict ourselves to the case $p = 1$, $q = 2$. In that case, the equations of motion are reduced to

$$\dot{C}_2 = [(1 - 2M_2 - 3M_2^2)A + 2B]S_2,$$

$$\dot{S}_2 = -(1 - 2M_2 - 3M_2^2 + 2B)C_2,$$

$$\dot{M}_2 = 2(-1 + A)C_2S_2.$$

Both north and south poles $(0, 0, \pm 1)$ make zero the equations; thus they are equilibria everywhere.

The meridian $S_2 = 0$ contains two equilibria. The coordinate M_2 is given by the roots of the second degree equation $(1 - 2M_2 - 3M_2^2 + 2B) = 0$, that is,

$$M_2^{(s+)} = \frac{1}{3}(-1 + \sqrt{4 + 6B}), \qquad \text{only for} \qquad -\frac{2}{3} \leq B \leq 2,$$

$$M_2^{(s-)} = \frac{1}{3}(-1 - \sqrt{4 + 6B}), \qquad \text{only for} \qquad -\frac{2}{3} \leq B \leq 0,$$

and C_2 is determined from the equation of the surface (1.5).

The meridian $C_2 = 0$ contains other two equilibria. M_2 is given by the roots of the equation $(1 - 2M_2 - 3M_2^2)A + 2B = 0$, that is,

$$M_2^{(c+)} = \frac{1}{3}(-1 + \sqrt{4 + 6B/A}), \qquad \text{only for} \qquad -\frac{2}{3} \leq B/A \leq 2,$$

$$M_2^{(c-)} = \frac{1}{3}(-1 - \sqrt{4 + 6B/A}), \qquad \text{only for} \qquad -\frac{2}{3} \leq B/A \leq 0,$$

and S_2 is obtained by solving the equation (1.5) for $C_2 = 0$ and M_2 each one of the above roots.

But for the particular case $A = 1$, there results that the two parallels

$$M_2^{(+)} = \frac{1}{3}(-1 + \sqrt{4 + 6B}), \qquad \text{only for} \qquad -\frac{2}{3} \leq B \leq 2,$$

$$M_2^{(-)} = \frac{1}{3}(-1 - \sqrt{4 + 6B}), \qquad \text{only for} \qquad -\frac{2}{3} \leq B \leq 0,$$

and C_2 and S_2 on the corresponding minor circle, make zero the equations; thus we have either none, one or two circles of no-isolated equilibria.

The partition of the parametric plane AB and the number of equilibria in each region are shown in Figure 3.1.

3.2. One quadratic term plus two linear ones. Let us take now the following Hamiltonian made by one quadratic term and two linear terms:

$$H = \frac{1}{2}C_2^2 + AC_2 + BM_2. \tag{3.2}$$

For this Hamiltonian (and as in the previous case, we take $p = 1$, $q = 2$), the equations of the motion are now

$$\dot{C}_2 = 2BS_2,$$

$$\dot{S}_2 = A(-1 + 2M_2 + 3M_2^2) + C_2(-1 - 2B + 2M_2 + 3M_2^2),$$

$$\dot{M}_2 = -2(A + C_2)\, S_2.$$

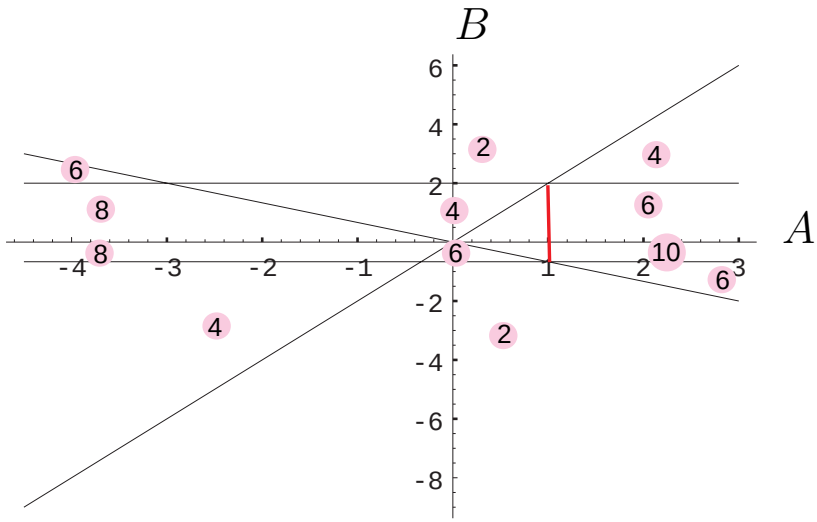

FIG. 3.1. *Parametric bifurcations for the Hamiltonian (3.1) and $p = 1$, $q = 2$. The vertical segment $A = 1$, $-2/3 \leq B \leq 2$ corresponds to the degenerate cases of non-isolated equilibria. The encircled numbers stand for the number of equilibria in the corresponding region.*

These equations enjoy the symmetry $(A, C_2, t) \mapsto (-A, -C_2, -t)$.

The south pole $(0, 0, -1)$ is equilibrium everywhere, while the condition for the north pole be equilibrium is $A = 0$.

For $B = 0$ we have a degeneracy, that is to say, a set of non isolated equilibria. Indeed, for $B = 0$, every point of the curve $C_2 = -A$ (and $|A| \leq R$), with S_2 and M_2 on the curve $S_2^2 + A^2 = (1 + M_2)^2(1 - M_2)$ is equilibrium. Besides, for $B = 0$, the points

$$\left(\pm\frac{4}{3}\sqrt{\frac{2}{3}}, 0, \frac{1}{3}\right)$$

are also equilibria.

For $B \neq 0$, the possible equilibria must lie on the meridian $S_2 = 0$. The other two coordinates of the equilibria must be the roots of the system

$$\left.\begin{array}{l} A(-1 + 2M_2 + 3M_2^2) + C_2(-1 - 2B + 2M_2 + 3M_2^2) = 0, \\ C_2^2 = (1 + M_2)^2\,(1 - M_2), \end{array}\right\}$$

or equivalently, M_2 must be a root of the equations

$$A(-1 + 2M_2 + 3M_2^2) \pm (-1 - 2B + 2M_2 + 3M_2^2)(1 + M_2)\,(1 - M_2)^{1/2} = 0,$$

and such that $-1 \leq M_2 \leq 1$.

A detailed analysis of the number of roots depending on the values of the parameters, gives a partition of the parametric plane A, B, that is represented on Figure 3.2. Note that any root of this equation for the sign $(+)$ and a value of A, is also a root for the sign $(-)$ and $-A$, which is a consequence of the symmetry of the equations of motion. The figure is a kind of deformation of the astroid found in case (2.3), although the variety of cases is much richer.

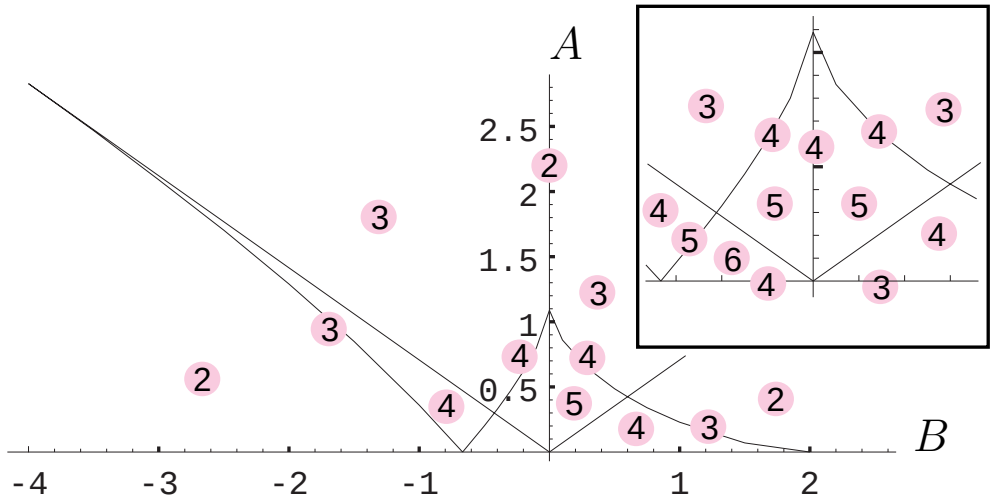

FIG. 3.2. *Parametric bifurcations for the Hamiltonian (3.2) and $p = 1$, $q = 2$. The segment $B = 0$, $-R \leq A \leq R$ corresponds to the degenerate case of non-isolated equilibria. The encircled numbers stand for the number of equilibria in the corresponding region (Note that we did not plot the symmetric part ($A < 0$)). The framed figure to the right is a zoom of the origin area.*

As an illustration, in order to see the evolution of the phase flow and how the different bifurcations appear, we fix the value $A = 0.2$, and will take several values of B. Since the equilibria are located on the meridian $S_2 = 0$, to visualize the location of the equilibria, we may plot the curves

$$C_2 = \pm(1 + M_2)^2 (1 - M_2), \qquad C_2 = -\frac{(-1 - 2B + 2M_2 + 3M_2^2)}{A(-1 + 2M_2 + 3M_2^2)},$$

and the points at which the curves cut each other are the equilibria.

From the analysis of the eigenvalues of the variational equations we determined the stability of the points. The evolution for several values of B along the straight line $A = 0.2$ as well as the stability are given in the Figure 3.3. The letters s and u stand for stable and unstable respectively.

Since the Figure 3.3 has a matricial form, we will refer to its different parts with the elements $F_{i,j}$ of a matrix F. For $B = -1.5$, there are only two equilibria, the south pole and one point near the north pole, both of them stable ($F_{1,1}$). At the value $B = -0.84596$, a new equilibrium appears ($F_{1,2}$) through a saddle-node bifurcation. Passed this value, the saddle-node bifurcation creates two points, one stable, the other unstable ($F_{1,3}$). The latter is approaching to the south pole as B increases. At $B = -0.500065$, a new saddle-node appear, but now in the negative part of C_2 ($F_{2,1}$). Again, this saddle-node bifurcation gives rise to two equilibria, one stable and the other unstable ($F_{2,2}$).

For $B = -0.2\sqrt{2}$, the unstable point that was approaching the south pole, merged with it, originating only one unstable point, and we notice also that there are two equilibria, both stable with almost the same coordinate M_2, and the remaining two equilibria, stable and unstable, have almost the same coordinate C_2 ($F_{2,3}$). Precisely, at $B = 0$, both have the same $C_2 = -A = -0.2$, but every point on the surface with

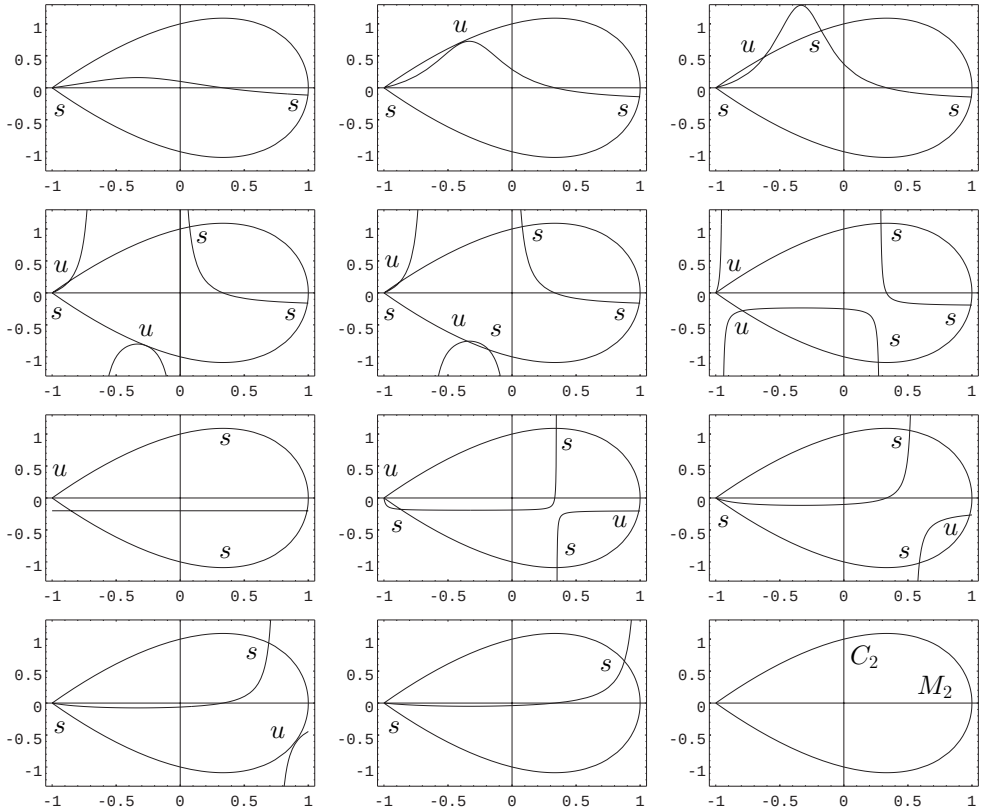

FIG. 3.3. *Evolution of the parametric bifurcations for the Hamiltonian (3.2) with* $p = 1$, $q = 2$ *and* $A = 0.2$. *From left to right and from top to botton, the values of* B *are: -1.5, -0.84596, -0.6; -0.500065, -0.49, -0.282843; 0.0, 0.03, 0.282843; 1.077455 and 2.2. The equilibria are located on the meridian* $S_2 = 0$.

$C_2 = -A$ and $B = 0$ is equilibrium. We have a degeneracy ($F_{3,1}$), and the bifurcation is of the *butterfly* type [6, 24].

Once $B = 0$ is passed, the degeneracy disappears and the butterfly bifurcation switches the stability of the two points, the equilibrium closest to the north pole that was stable becomes unstable, and the one closest to the south pole becomes stable ($F_{3,1}$). But soon ($B = 0.2\sqrt{2}$), this point will merge with the south pole, that will be now stable ($F_{3,2}$) and will maintain its stability as well as the point with $C_2, M_2 > 0$ does for greater values of B. On the contrary the remaining two points ($C_2 < 0$) will approach one another ($F_{3,3}$) until both melt into only one ($F_{4,1}$) through a new saddle-node bifurcation at $B = 1.077455$ and then, disappears for greater values of B.

In the case here considered, since all equilibria are placed on the meridian $S_2 = 0$, it has been easy to determine them. However, in other cases, the finding of the equilibria would be more complex. It is precisely for those situations that we should use other tools. The traditional technique to build the phase portrait is to plot the trajectories by numerically integrating the differential equations. Another faster procedure is the so called *painting Hamiltonians* technique [5], that consist of assignning a color

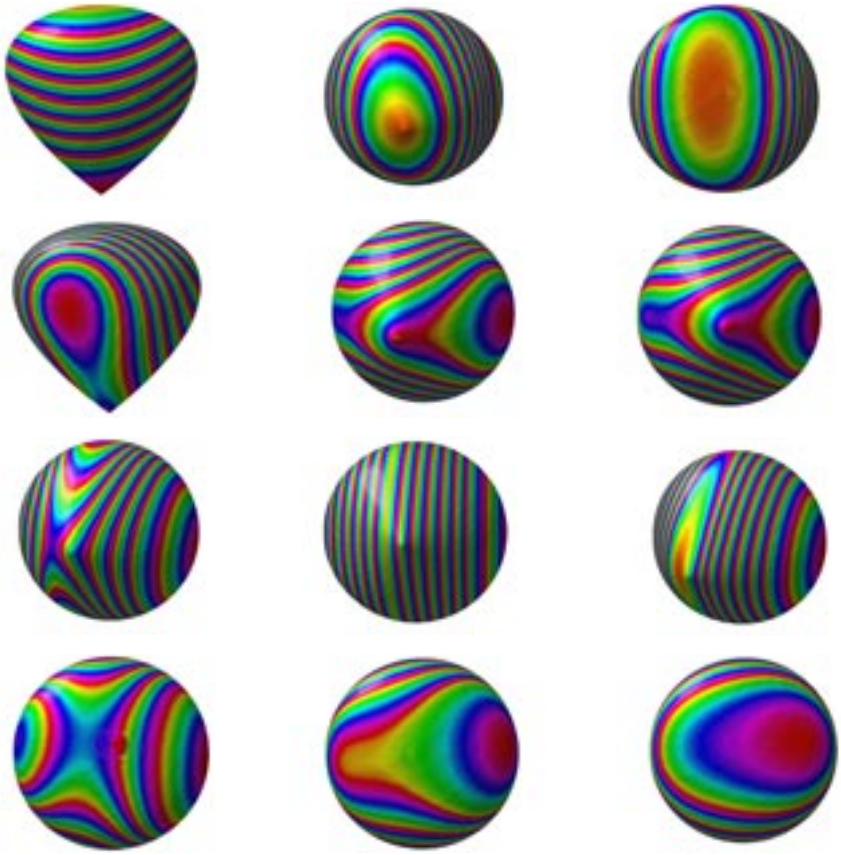

FIG. 3.4. *Phase portraits for different values of the parameter B. First row, two equilibria (case $F_{1,1}$ of Figure 3.3); different points of view. Second row, corresponds to cases$F_{1,3}$, and $F_{2,1}$, $F_{2,2}$ (a saddle-node bifurcation). Third and fourth rows correspond to the sequence $F_{2,3}$ to $F_{4,2}$; first (3th row), a butterfly bifurcation occurs through a degeneracy (view from the south pole). Then, two equilibria, one stable and other unstable, disappear through a new saddle-node bifurcation (last row, view from the north pole)*

palette to levels of energy and thus, the level contours of the Hamiltonian (3.2) over the surface (1.5).

Although the *painting hamiltonians* technique was elaborated for parallel computers to produce high resolution pictures [5], we take advantage of the magnifications to highlight the low gradient areas when it is necessary. We have produced the adequate software with Mathematica in order to implement this technique on a personal computer and interacting the graphics possibilities of Mathematica with its package Graphics Visualizer. By so doing, once fixed the parameters A and B, we obtain a 3D graphics, that we may rotate by clicking and dragging the cursor on the screen. In Figure 3.4 we present some of the views for several parameters in order to illustrate the type of bifurcations produced. Several 3D pictures can be found at `http://gme.unizar.es/paginas/avellanas.html`, that can be rotated on the screen by clicking and dragging the cursor.

4. Conclusions. For parametric quadratic Hamiltonians with the Poisson structure (1.4), the loss of spherical symmetry with respect to the classical structure (1.1),

makes that the number of independent parametric cases be different from the classical one. In the same manner, the number of equilibria and the parametric bifurcations in the phase space are different. The type of bifurcations and the variety of them is much richer.

Acknowledgments. Supported by the Spanish Ministry of Science and Technology (Projects # ESP2002-02329 and # BFM2003-02137).

REFERENCES

[1] R. Abraham and J. E. Marsden, *Foundations of Mechanics*, Second ed., Benjamin/Cummings, Reading, MA, 1980.

[2] V.I. Arnold , *Dynamical Systems III* Springer-Verlag, Berlin, 1988.

[3] V.I. Arnold , *Mathematical Methods of Classical Mechanics* Second ed., Springer-Verlag, New York, 1989.

[4] G. Contopoulos and M. Moutsoulas, *Resonance cases and small divisors in a third integral of motion II*, Astronomical Journal, 70 (1966), pp. 687–698.

[5] S. Coffey, A. Deprit, E. Deprit, and L. Healy, *Painting the phase space portrait of an integrable dynamical system*, Science,247 (1990), pp. 833–836.

[6] D. David, D.D. Holm and M.V. Tratnik, *Integrable and chaotic polarization dynamics in nonlinear optical beams*, Phys. Lett. A, 137(1989), pp. 355–364.

[7] D. David, D.D. Holm and M.V. Tratnik, *Hamiltonian chaos in nonlinear optical polarization dynamics*, Phys. Rep.,187 (1990), pp. 281–367.

[8] A. Deprit, *The Lissajous transformation I. Basics*, Celestial Mechanics and Dynamical Astronomy, 51 (1991), pp. 201–225.

[9] A. Deprit and A. Elipe, *The Lissajous transformation II. Normalization*, Celestial Mechanics and Dynamical Astronomy, 51 (1991), pp. 227–250.

[10] A. Deprit and A. Elipe, *Complete reduction of the Euler-Poinsot problem*, Journal of the Astronautical Sciences, 51 (1993), pp. 603–628.

[11] A. Elipe, *Complete reduction of oscillators in resonance p:q'*, Physical Review E, 61 (2000), pp. 6477–6484.

[12] A. Elipe, M. Arribas and A. Riaguas, *Complete analysis of bifurcations in the axial gyrostat problem*, Journal of Physics A: Mathematics and General, 30 (1997), pp. 587–601.

[13] A. Elipe and A. Deprit, *Oscillators in resonance*, Mechanics Research Communications, 26 (1999), pp. 635–640.

[14] A. Elipe and S. Ferrer, *Reductions, relative equilibria and bifurcations in the generalized van der Waals potential: Relation to the integrable cases* , Phys. Rev. Lett., 72 (1994), pp. 985–988.

[15] A. Elipe, B. R. Miller and M. Vallejo, *Bifurcations in a non symmetric cubic potential*, Astronomy and Astrophysics, 300 (1995), pp. 722–725.

[16] D. Farrelly, *Lie algebraic approach to quantization of nonseparable system with internal nonlineal resonance*, Journal of Chemical Physics, 85 (1986), pp. 2119–2131.

[17] D. Farrelly and T. Uzer, *Semiclassical quantization of slightly nonresonant systems: Avoided crossings, dynamical tunneling, and molecular spectra*, Journal of Chemical Physics, 85 (1986), pp. 308–318.

[18] E. Fermi, J. Pasta and S. Ulam, *Studies of nonlinear problems I*, Los Alamos Scientific Laboratory Report, LA-1940 (1955), 20 pp.

[19] J. Frauendiener, *Quadratic Hamiltonians on the unit sphere*, Mechanics Research Communications, 22 (1995), pp. 313–317.

[20] H. Friedich and D. Wintgen1989, *The Hydrogen atom in a uniform magnetic field*, Physics Reports, 183 (1989), pp. 37–79.

[21] M. Kummer, *On Resonant Hamiltonian systems with finitely many degrees of freedom*, Local and Global Methods in Nonlinear Dynamics, (Sanz *et al.* Ed.), Lecture Notes in Physics, 252 (1984), pp. 19–31.

[22] V. Lanchares and A. Elipe, *Biparametric quadratic Hamiltonians on the unit sphere: complete classification*, Mechanics Research Communications, 21 (1994), pp. 209–214.

[23] V. Lanchares and A. Elipe, *Bifurcations in biparametric quadratic potentials*, Chaos, 5 (1995), pp. 367–373.

[24] V. Lanchares and A. Elipe, *Bifurcations in biparametric quadratic potentials. II*, Chaos, 5 (1995), pp. 531–535.

[25] V. Lanchares, M. Iñarrea, J. P. Salas, J. D. Sierra and A. Elipe, *Surfaces of bifurcation in a triparametric quadratic Hamiltonian*, Physical Review E, 52 (1995), pp. 5540–5548.

[26] A. J. Lichtenberg and M. A. Lieberman, *Regular and Stochastic Motion* Applied Mathematics Sciences **38** (Springer-Verlag, New York).

[27] J. E.Marsden and T. S. Ratiu, *Introduction to Mechanics and Symmetry,* Text in Applied Mathematics, 17 (1994) (Springer, New York).

[28] B. Miller, *The Lissajous transformation III. Parametric bifurcations*, Celestial Mechanics and Dynamical Astronomy, 51 (1991), pp. 251–270.

[29] J. Moser, *Regularization of Kepler's problem and the averaging method on a manifold*, Communications on Pure and Applied Mathematics, XXIII (1970), pp. 609–636.

[30] T. Uzer, D. Farrelly, J. Milligan, P. Raines and J. Skelton, *Celestial Mechanics on a Microscopic Scales*, Science, 253 (1991), pp. 42–48.